Fueling Control for Improving Plasma Performance in Heliotron J

T. Mizuuchi 1), S. Kobayashi 1), S. Yamamoto 1), K. Mukai 2), H. Okada 1), S. Ohshima 3), M. Takeuchi 1), T. Minami 1), K. Nagasaki 1), H.Y. Lee 2), K. Nomura 2), M. Suwa 2), K. Yamamoto 2), H. Yashiro 2), H. Yoshino 2), N. Nishino 4), Y. Nakashima 5), K, Hanatani 1), Y. Nakamura 2), S. Konoshima 1), F. Sano 1)

1) Institute of Advanced Energy, Kyoto Univ., Gokasho, Uji, 611-0011 Japan.
2) Graduate School of Energy Science, Kyoto Univ., Gokasho, Uji, Japan.
3) Kyoto Univ. Pioneering Research Unit for Next Generation, Gokasho, Uji, Japan.
4) Graduate School of Engineering, Hiroshima Univ., Higashi-Hiroshima, Japan.
5) Plasma Research Center, Univ. of Tsukuba, Tsukuba, Japan.

E-mail contact of main author: mizuuchi@iae.kyoto-u.ac.jp

Abstract. This paper discusses the effects of the fueling control on plasma performance in Heliotron J. Supersonic Molecular Beam Injection (SMBI) fueling is successfully applied to Heliotron J plasma. A supersonic H_2-beam is effective to increase fueling efficiency and make a peaked profile. In a combination heating condition of ECH and Co-NBI, the stored energy reached about 50% higher value than the maximum value achieved so far under the similar heating condition with conventional gas-puff fueling. Local fueling with a short pulse by SMBI can increase the core plasma density avoiding the degradation due to the edge cooling. A large increment of plasma stored energy after a short pulse intense gas fueling from a conventional piezoelectric-valve system has been observed in NBI (or NBI+ECH) plasma. The physics under the observation would give us a new insight into more preferable plasma operation conditions.

1. Introduction

Fueling/recycling control is one of the key issues to obtain high density and high performance plasma in magnetic confinement devices from two aspects; (1) profile control of core plasma and (2) reduction of neutrals in the peripheral region. Core fueling by ice pellets is well known as a technique to realize favorable fueling from these aspects. The pellet system is, however, complicated and it is not easy to make pellets small enough for density control in medium or small sized devices. A supersonic molecular-beam injection (SMBI) technique is, on the other hand, considered to be not only an effective fueling method for deeper penetration of neutral particles into the core plasma compared to the conventional gas-puffing (GP) [1] but also an effective edge modification technique in fusion devices [2, 3, 4].

In Heliotron J, high-pressure SMBI has been examined as a fuelling method. In a combination heating condition of ECH and Co-NBI, the stored energy reached ~ 4.5kJ, which is about 50% higher than the maximum one achieved so far under the similar heating condition with conventional gas-puff fueling in Heliotron J [5]. In addition, a large increment of plasma stored energy after a short pulse of intense GP has been observed in recent NBI experiments in Heliotron J [6].

This paper discusses the effects of fueling control on plasma performance in Heliotron J.

2. Experimental Set-up

Heliotron J [7, 8] is a medium sized helical device ($\langle R_0 \rangle / \langle a_p \rangle$ = 1.2/0.17m, $\langle B_0 \rangle \leq$ 1.5T) based on the helical-axis heliotron concept [9, 10] with an L/M = 1/4 helical coil, where L and M are the pole number of the helical coil and its helical pitch number, respectively. The initial

hydrogen or deuterium plasma is produced by using second harmonic X-mode ECH (70GHz, < 0.40MW). The hydrogen beam is injected for NBI experiments by using one or two tangential beam-lines (BL-1 and BL-2. The acceleration voltage is < 30kV and the beam power is < 0.7MW/beam-line). In this experiment, ICRF was not applied.

Figure 1 schematically shows a layout of main heating, fueling and some diagnostic equipment for this experiment. For density control, a gas-puffing system with four piezoelectric valves is usually used, which are installed at the inboard-side ports at ≈ 90° intervals around the torus (indicated by "Gas" in Fig. 1(top)). Due to the space limitation, the nozzles of these valves do not directly see the plasma. The amount of H (or D) atoms from the GP system is pre-programmed to control the line-averaged density. Two SMBI systems of hydrogen are equipped on two horizontal outboard-side ports (the port number: #3.5, #11.5). The SMBI system at #11.5 consists of a fast solenoid-valve with a short (~ 4 mm) conic-nozzle. The diameter of its orifice is 0.2 mm^{ϕ} for this experiment. To reduce the stray field effect on the fast valve action, a soft-magnetic-iron cylinder covers it as a magnetic shield. The other system at #3.5 consists of a fast piezoelectric valve with a short conic-nozzle (0.2 mm^{ϕ} orifice). In front of the #3.5-SMBI nozzle, a movable shutter plate is installed to protect a viewing window at the same port. The amount of H atoms injected with these SMBIs is controlled by changing the pulse width of each SMBI valve under a fixed plenum pressure (P_{pl} ~1-2 MPa).

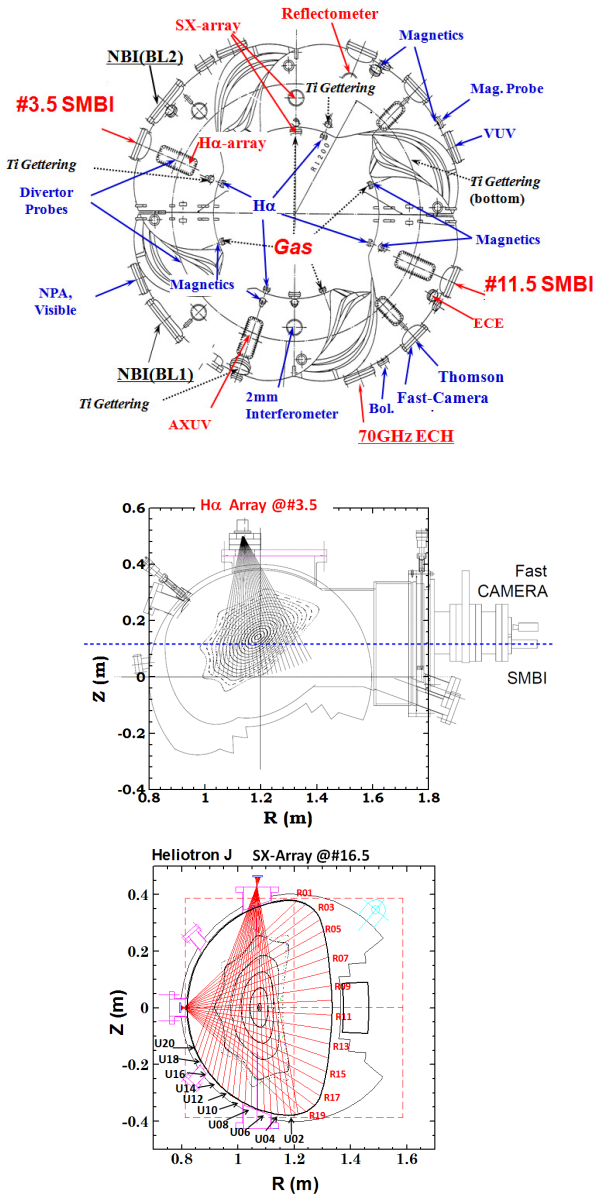

Fig. 1 *Experimental Set-up. A layout of main heating, fueling and diagnostic equipments (topt). Relation between the flux surfaces (the standard configuration [8]), sight-lines of Hα-array at #3.5 (middle) and sight-lines of two SX-arrays at #16.5 (bottom).*

The speed of injected H_2-beam is evaluated by a "time of flight" method, where the distance from the nozzle to the last closed flux surface (LCFS) is divided by the delay time from the SMBI trigger to the start of Hα increase monitored at almost the same toroidal position with the injector. The beam speed of 1.3-1.6 km/s is evaluated for P_{pl} ~ 1.0-1.5 MPa [11]. This value is also confirmed by a time of flight method with a fast ionization gauge in a test chamber without plasma.

3. Effects of SMBI fueling

Figure 2 shows an example of time responce of some plasma parameters for an ECH+NBI discharge under the standard (STD) configuration [8] of Heliotron J. Here, the line averaged electron density $\bar{n}_e$ is mainly controlled by using multiple #11.5-SMBI pulses (indicated as sawteeth-like Hα at #11.5) with moderate injection rate of H_2 in addition to almost constant low flow-rate D_2 GP. In response to the SMBI pulses, $\bar{n}_e$ is increased and the increase of the stored energy W_p follows with a small delay. Second-harmonic ECE from the plasma core ECE_{67GHz}, which is an indicater of the change of core electron temperature in this density range, drops just after each SMBI pulse and tries to recover between SMBI pulses, but it gradually decreases as increase of $\bar{n}_e$. The time delay in W_p response would be explained by the temperature drop just after SMBI pulses. Almost no response in Hα monitored at #3.5 section (not shown. ~ 180° toroidally apart from the injection port.) indicates the direct effect of injected neutrals is localized near the injection port.

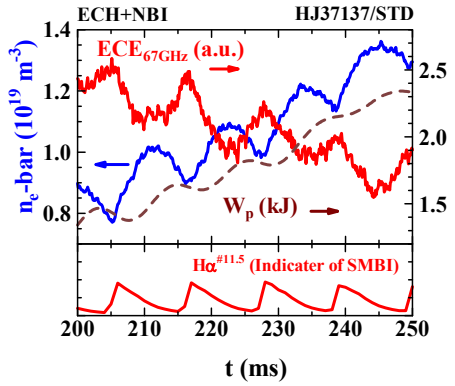

Fig. 2 *Responses of the line averaged density, ECE intensity from the core region and the stored energy caused by multiple SMBI for an ECH+NBI plasma. During this time span, the heating condition is almost kept constant.*

An advantage for the SMBI method for the fueling scenarios becomes clear when the dependence of W_p on $\bar{n}_e$ is compared. Figure 3(a) and (b) show the time history of some plasma parameters for ECH(~ 0.35 MW) + Co-NBI(~ 0.6 MW) plasmas with two different fueling scenarios in the STD configuration; (a) with a single intense SMBI and (b) short and

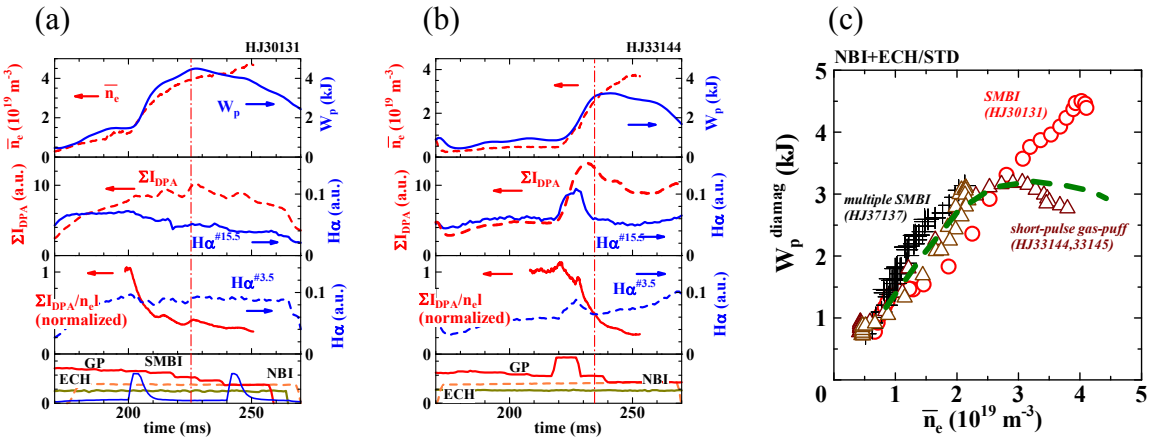

Fig. 3 *(a) Time traces of $\bar{n}_e$, W_p, H_α (at #3.5 and #15.5), ΣI_{DPA} and $\Sigma I_{DPA}/n_e l$ for an ECH+NBI discharge with a single intense SNBI. Here, ΣI_{DPA}, the summation of ion-saturation currents measured by a Langmuir probe pins of a divertor-probe-array at #3.5-section is shown as an indicator of change in particle loss [12]. (b) Similar traces for an ECH+NBI discharge with a short pulse of intense GP. (c) Dependence of W_p on $\bar{n}_e$ under the same condition of ECH+NBI with a single intense SMBI (○), a series of moderate SMBI (+) and a short and intense GP (△), respectively. The green dashed-line is the upper envelop of the data for conventional GP cases.*

intense GP. Figure 3(c) shows $\bar{n}_e$–W_p dependence for different fueling scenarios. For normal GP case, the atainable W_p in this heating condition under the STD configuration becomes saturated around ~ 3 kJ as increase $\bar{n}_e$ or decreased in higher-$\bar{n}_e$ region (> 2.5×10^{19} m^{-3} in this heating condition) [12]. This is probably due to the edge cooling caused by excess neutrals. When $\bar{n}_e$ is gradually increased by a series of moderate SMBI pulses, slightly higher W_p is observed in lower density region than that in the normal GP case. When $\bar{n}_e$ is increased by a single intense SMBI, W_p increases beyond the saturation level for the GP case and reached about 50 % higher value than the maximum achieved under the normal GP fueling. Although the short and intense GP can produce a rapid increase of $\bar{n}_e$ (△) similar to that in the SMBI case, W_p is saturated at almost the same level as the normal GP case [5].

Since the SMB speed itself is not so fast compared to that for H_2 introduced by normal GP, the key points of SMBI, which cause the peculiar plasma performance in SMBI, should be its directional motion of the injected gas and the small area of plasma-beam interaction. Judging from the visible-light image measured with a fast camera [13], the core part of H_2-beam should be less than ~ 10 cm near the LCFS. For the normal GP case, on the other hand, a previous Monte-Carlo simulation of neutral particles [14] indicates that the neutrals from GP expands widely in toroidal and poloidal directions. Therefore, the high neutral density area,

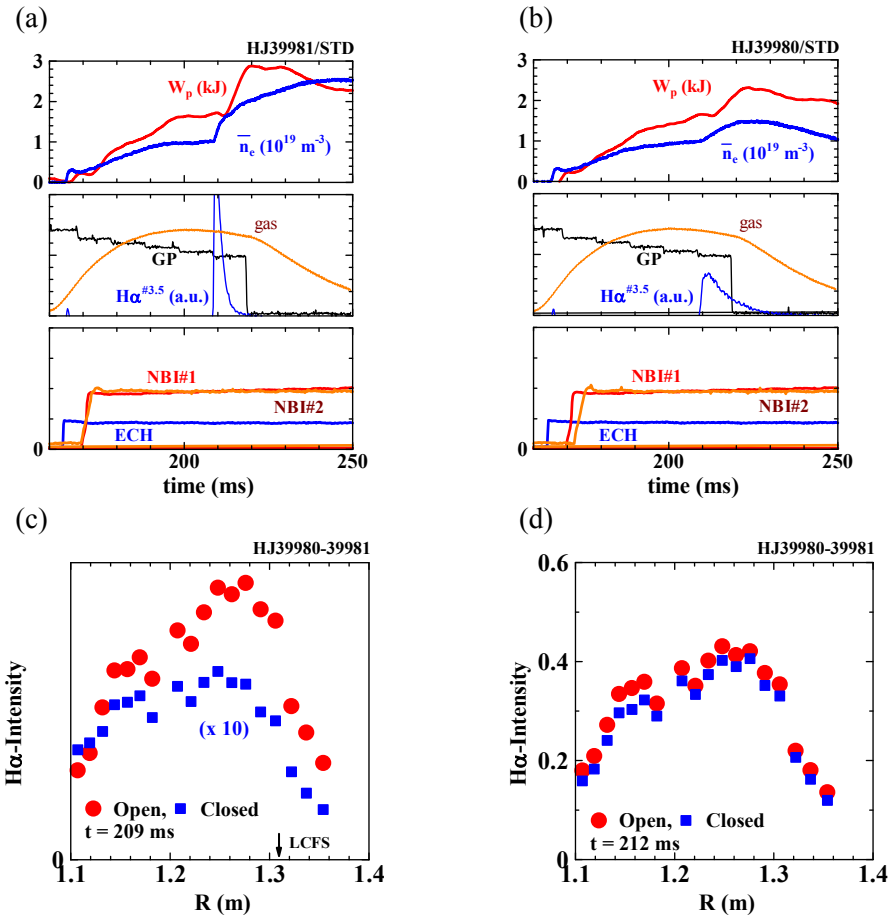

Fig. 4 *Top: Time traces of line-averaged density, stored energy for ECH+NBI plasmas between two cases of open (a) and closed (b) conditions of the shutter in front of SMBI. Bottom: Chord profiles of Hα at the SMBI section (#3.5) for the open shutter case (●) and the closed case (■) at two different timings, 209 and 212 ms.*

where the plasma performance might be degraded through the increase of CX-loss, convection, etc., is quite small and localized in SMBI.

Direct comparison between the beam (directional) gas injection and non-directional gas injection was performed by using the movable shutter plate in front of the #3.5-SMBI. Figures 4 shows time traces of W_p and $\bar{n}_e$ and Hα at #3.5 (indicating the SMBI timing, $t \approx$ 208.5 ms) for two discharges under the same heating condition; the shutter is open (a) and closed (b). As shown in the figures, $\bar{n}_e$ shows rapid increase just after SMBI and then gradually increases up to ~ 2.6×10^{19} m^{-3} during ~30 ms in the directly injected case (the open shutter case). The stored energy also shows rapid increase with a slight delay, keeps the elevated value for ~10 ms and then starts to decrease when the increase of $\bar{n}_e$ becomes saturated. In the case of closed shutter, on the other hand, the increases of $\bar{n}_e$ and W_p are slow and mild. The density already saturates at ~1.4×10^{19} m^{-3} and starts to decrease at ~15 ms after SMBI. Since the amount of injected gas is the same for these two cases, the difference of the attainable $\bar{n}_e$ after the SMBI indicates the effectiveness of SMBI in the over-all fueling efficiency perhaps including the confinement improving effect.

When the shutter is closed, the SMBI beam hits the plate and then H_2 molecules diffuse to the plasma, which is suggested by a low and slow response of $H\alpha^{\#3.5}$ shown in Fig. 4(a) and (b). More directly, the chord profile of Hα-intensity measured with the Hα-array at #3.5 is compared in Fig. 4(c) and (d) for two timing. Just after SMBI (Fig. 4(c)), very strong (> ×10) emission is observed for sight-lines crossing the beam-line inside the LCFS (R < 1.31 m). On the other hand, only 3 ms later timing (Fig. 4(d)), almost the same chord profile and intensity are observed for both the cases. These observations indicate that the injected beam well penetrate to core plasma region in the open shutter case. Similar difference in the SMBI

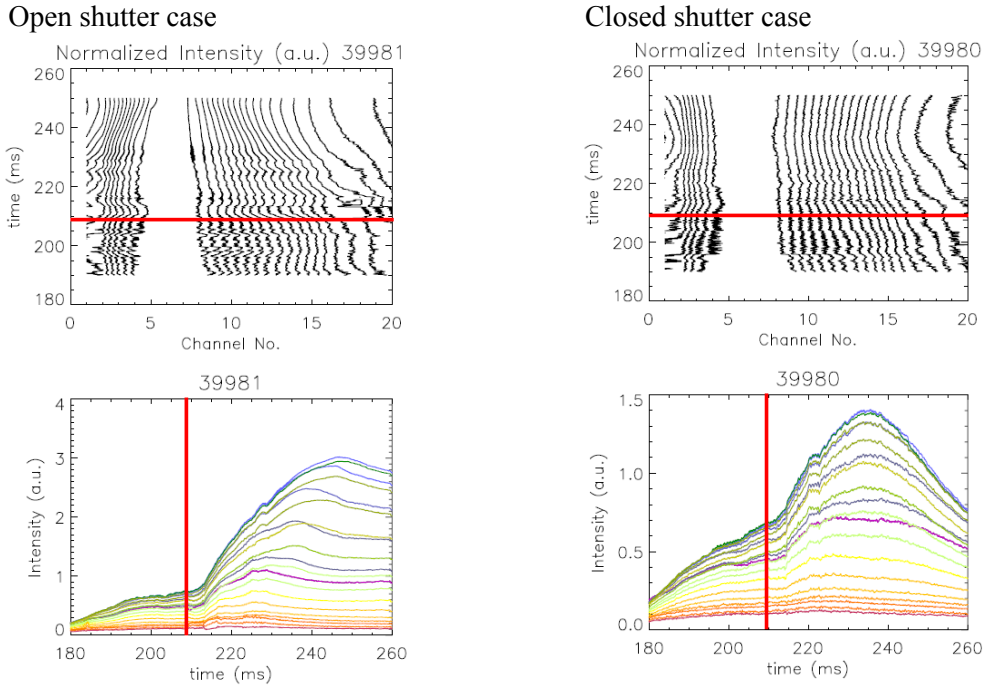

Fig. 5 *Normalized chord profile of SX emission observed from a top port at #16.5 for the open shutter case (left) and for the closed shutter case (right). The figures in top line shows the contour plots of the intensity normalized by the maximum value at each timing. The figures in bottom line shows the time traces of each channel. Red lines indicate the SMBI timing.*

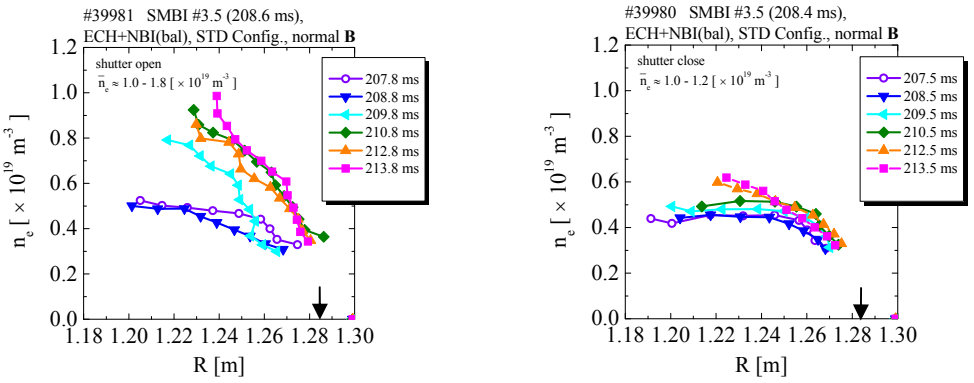

Fig. 6 *.Density profile measured with a microwave reflectometer for ECH+NBI plasmas (see Fig. 4) in two cases of open (left) and closed (right) conditions of the shutter. The sight-lines are shown in Fig. 1. The arrow in the figure indicates the LCFS position. (R_0 ≈1.12 m)*

response is also observed in the SX emission profile. Figure 5 (bottom) shows the time history of SX emission measured from a top port at #16.5 for these two cases, where difference in color corresponds to different chords of the SX-array. In Fig. 5 (top), to make clear the difference in the response, the contour plot of intensity profile normalized by the maximum value at each time slice are also shown. In the open shutter case, the drop of emission is clearly observed for ~ 5 ms after SMBI even in the center chord. Moreover, the change in contour plot suggests peaking of the profile. On the other hand, in the closed case, these changes are not so clear. These observations support that the H_2-beam from SMBI can penetrate deeply enough to the inside of LCFS. As for the effect on the density profile, Fig. 6 shows the change of density profile for these two discharges measured with a microwave reflectmeter at #15.5 section [15]. In the open shutter case, the density profile, which is rather flat before SMBI, rapidly changes to a very peaked one after SMBI, while the profile change is slow and mild in the closed shutter case. Taking account the increase in density, the observed change in the SX emission intensity and its chord profile observed just after SMBI would suggest the decrease of electron temperature and peaking of its profile.

Since the deposition rate and/or deposition profile of NBI power should depend on the target plasma (density/temperature) profile and neutral density around the plasma, the modification of plasma profile and reduced neutral density condition realized by SMBI might have preferable effects on NBI plasma heating. From this point of view, a comparative study was performed for NBI plasma. Here, after plasma initiation with a short pulse of ECH, the first NBI is injected and sustains target plasma. After that, the second NBI is injected. Figure 7 shows the time trace of $\bar{n}_e$ and W_p for with and without SMBI, which is injected just before the second NBI. (The SMBI timing is indicated a sharp raise of $H\alpha^{\#3.5}$ in Fig. 7(a).) As shown in

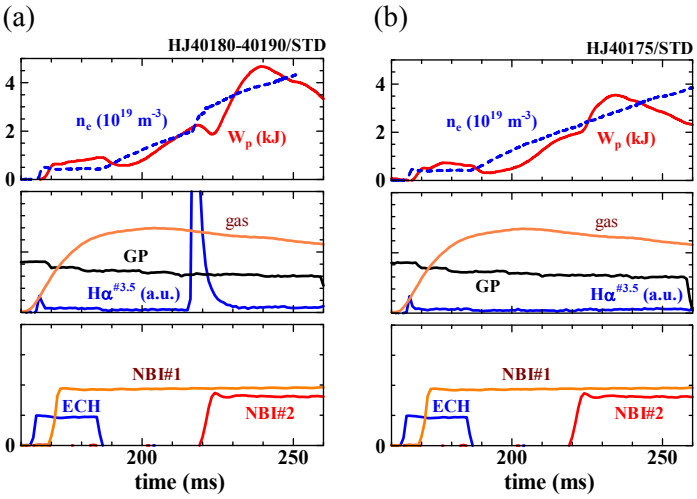

Fig. 7 Comparison of plasma performance between with (a) and without (b) SMBI for NBI heating.

Fig. 7(b), due to the second NBI, W_p starts to increase but it turns over at $t \sim 220$ ms, where $\bar{n}_e$ is $\sim 3\times10^{19}$ m^{-3}, even though NBIs are still injected. As shown in Fig. 7(a), on the other hand, $\bar{n}_e$ steps up just after SMBI as usual. Although W_p drops in a short duration after SMBI, it rapidly increases in the second NBI phase to reach a factor ~1.3 higher value compared to the no SMBI case in this experimental condition.

4. Fueling by a short-pulse intense GP

A large increment of plasma stored energy after a short pulse intense GP has been observed in NBI (or NBI+ECH) plasma. Although this kind of discharge was initially observed in NBI-only plasmas under a high bumpiness ε_b with relatively small toroidicity ε_t configuration ($\varepsilon_t/\varepsilon_h$, $\varepsilon_b/\varepsilon_h$) = (0.77, -1.05) at the magnetic field of 1.32 T [6], where ε_t is helicity, the similar phenomena can be also observed in NBI+ECH plasmas and in the STD configuration.

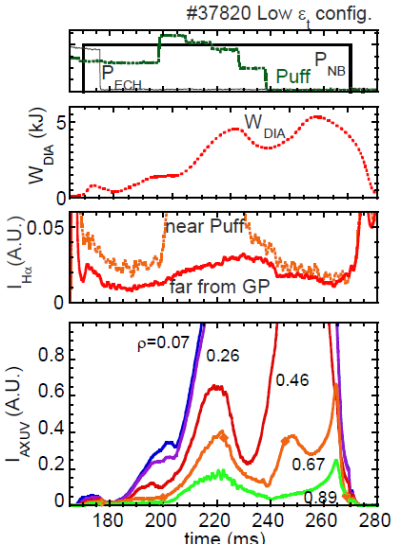

Fig. 8 *Time traces of plasma parameters in a shot-pulse intense GP scenario.*

Figure 8 shows an example of time traces of several plasma parameters obtained in such a condition, where a total injection power from two NBIs are around 1 MW. Although the increment in W_p is observed after a short-pulse intense GP ($t \sim 200$ ms), W_p starts to decrease during the heating pulse. As suggested by the decrease of the emission measured with an 1μm^t-Al filtered AXUV array at #7.5 section, this decrease of W_p is probably due to the cooling in the outer region of plasma ($\rho > 0.4$) caused by excess fueling by analogy with that discussed in previous section. However, the interesting point is the fact that W_p started to increase again at $t \sim 235$ ms and finally reached to over 5 kJ, which is higher than the first peak of W_p. Rapid increase in the edge AXUV intensity in the same timing might suggest the recovery of the energy balance in the edge region. Moreover, it is suggested that profile change in the density or temperature is caused after the intense GP. As a change of AXUV chord profile, the change in the intensity gradient around ρ =0.4-0.7 is remarkable after the intense GP.

This operation mode, however, seems to be very sensitive to the amount of GP. The change of the bright ring radius around the plasma in the tangential visible-light image suggests the shrink of the effective plasma radius from the edge and expansion from the core corresponding the decrease and increase W_p in this kind of operation. When the gas amount is too much, the energy balance in the center of the plasma is broken and the discharge is completely terminated without recovering. On the other hand, in the case of a “right” fueling condition, the plasma in the center region can survive the radiation collapse propagated from the edge region and can start a new discharge mode with more preferable plasma profile.

5. Summary

The optimization study of gas fueling scenario has been performed to control the plasma profile, resulting in high performance plasma formation in Heliotron J.

SMBI fueling is successfully applied to Heliotron J plasma. A supersonic H_2-beam is effective to increase fueling efficiency and make a peaked profile. In a combination heating condition of ECH and Co-NBI, the stored energy reached about 50% higher value than the maximum one achieved so far under the similar heating condition with conventional gas-puff fueling in Heliotron J. However, under conventional gas-puff fueling, probably due to the edge cooling caused by excess neutrals in wider area of plasma surface, the stored energy becomes saturate or decreased. Local fueling with a short pulse by SMBI can increase the core plasma density avoiding the degradation due to the edge cooling. Higher density and peaked profile of a target plasma is preferable for NBI since both of the power absorption rate and the global confinement time are expected to increase in such target plasma. To use the SMBI method more effectively to improve plasma performance or to expand the attainable plasma parameter range, more detailed studies and refinement of the SMBI system including an effective pumping system or recycling control are necessary.

A large increment of plasma stored energy after a short pulse intense GP has been observed in NBI (or NBI+ECH) plasma. Although this operation mode seems to be very sensitive to the amount of GP and is found to be an impressive way of improving plasma performance, the physics under the observation would give us a new insight into more preferable plasma operation conditions.

Acknowledgements

The authors are grateful to the Heliotron J supporting group for their excellent arrangement of the experiments. The authors give special thanks to Profs. L. Yao, Q.W. Yang and their colleagues in Southwestern Institute of Physics for kind instruction of SMBI experiments and fruitful discussions. This work is performed with the support and under the auspices of the JSPS-CAS Core University Program, the Collaboration Program of the Laboratory for Complex Energy Processes, IAE, Kyoto University, the NIFS Collaborative Research Program (*NIFS10KUHL030, etc.*) and the NIFS/NINS project of Formation of International Network for Scientific Collaborations, as well as the Grant-in-Aid for Sci. Research.

Reference

[1] YAO L., in “New Developments in Nuclear Fusion Research” (Nova Sci. Pub., 2006)) pp. 61-87.
[2] YAO L. and BALDZUHN J., Plasma Sci. Tech. **5**, 1933 (2003) .
[3] GIRUZZI G., et al., Nucl. Fusion **49**, 104010 (2009).
[4] TAKENAGA H., et al., Nucl. Fusion **49**, 075012 (2009).
[5] MIZUUCHI T., et al., Contrib. Plasma Phys. **50**, 639 (2010).
[6] KOBAYASHI, S., et al., in Proc. 37th EPS meeting (Dublin, 2010), P1-1053.
[7] SANO F., et al., J. Plasma Fusion Res. SERIES 3, 26 (2000).
[8] OBIKI T., et al., Nucl. Fusion **41**, 833 (2001).
[9] WAKATANI M., et al., Nucl. Fusion **40**, 569 (2000).
[10] YOKOYAMA M., et al., Nucl. Fusion 40, 261 (2000).
[11] MIZUUCHI T., et al., in Proc. 19th PSI Conference (San Diego, 2010) P2-70.
To be published in J. Nucl. Mater.
[12] MIZUUCHI T., et al., J. Plasma Fusion Res. 81, 949 (2005).
[13] NISHINO N., et al., in Proc. 19th PSI Conference (San Diego, 2010) P2-68.
To be published in J. Nucl. Mater.
[14] KOBAYASHI S., et al., 31st EPS Conf. Plasma Phys. (London, 2004) ECA Vol.28G, P-5.097.
[15] MUKAI K., et al., Contrib. Plasma Phys. **50**, 646 (2010).